Malaysian NANO-An International Journal

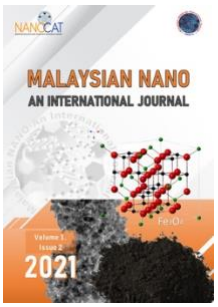

Research Article

Received 15th September 2021
Revised 9th November 2021
Accepted 29th November 2021

DOI:
https://doi.org/10.22452/mnij.vol1no2.5

Corresponding ***authors:***
rozalina@um.edu.my,
cheelong@gmail.com

Fabrication and Characterization of Single and Bimetallic Non-Alloyed Nanoparticles

M. N. S. M. Ismail[a], R. Zakaria[b], C. L. Tan[b*]

[a]*Institute for Advanced Studies (IAS), University of Malaya, 50603 Kuala Lumpur, Malaysia.*
[b]*Photonic Research Centre (PRC), Faculty of Science, University of Malaya.*

Abstract

We have demonstrated the fabrication of single and bimetallic Au and Ag nanoparticles on SiO_2 substrate for light trapping application. Those nanoparticles were obtained by depositing 6nm and 8nm Au while 8nm and 10nm of Ag on SiO_2 substrate. Then, the dewetting process takes place at 600^{o}C for Au and 500^{o}C for Ag. The particle distribution is quite non-uniform, making the shifting effect unclear and different from the previous result. However, the absorption effect of the BNNPs can be observed in this work, where it shows significantly broader peak spectra compared to both single Au and Ag NPs. This makes the BNNPs is the best candidate for selective detection sensors.

Keywords*:* SiO_2; Nanoparticles; Au; Ag; Sensors

1. Introduction

The study on plasmonic metal nanoparticles (NPS) has been intensively ongoing and attracted many researchers' interest. The light absorption involved applications such as photocatalysis (Wang, Huang, Dai, & Whangbo, 2015), optical sensing (Canfarotta, Whitcombe, & Piletsky, 2013; Nayeri,Moradinasab, & Fathipour, 2018), and optoelectronics (Rogach, 2000). In addition to the plasmonic electronic effects, this research focus on the enhancement of the photogeneration rate, the plasmon-induced "hot electrons," and improved conductivity of the hybrid nanostructure, which plays an essential role to enhance the photocatalytic reactions and the performance of photoelectric devices (Clavero, 2014; Ward & Bard, 1982).

Gold (Au) and silver (Ag) nanoparticle will be used in this research since they have strong scattering or absorption of light, which will give ease in monitoring light signals and also have a sensitive spectral response to the local environment (Lee & El-Sayed, 2006). Besides, this nanoparticle, especially gold, will have an excellent surface plasma resonance. The enhancement strongly depends on the size, shape, inter-particle interaction, dielectric properties, and the local environment of the nanoparticle (Ghosh & Pal, 2007). Instead of the light-trapping made by those single nanoparticles, they somehow exhibit a narrow plasmon-enhanced spectrum (Aroca, 2013). Thus, to improve the light absorption over the broad spectrum, we propose using bimetallic non-alloyed NPs (BNNPs) nanoparticles to study the effect on light trapping. Previously, Au-Ag BNNPs have enhanced the SERS on Si-film and c-Si substrate (Tan, Lee, & Lee, 2015). Results show that the SERS for Au-Ag BNNPs is 2.9 times higher than on Ag NPs on a similar substrate. Besides, a study also shows that Au-Ag BNNPs give broader surface plasma spectra than the single NPS itself (Yang, Shi, Kawamura, & Nogami, 2008).

Here, in this paper, we propose fabricating single and bimetallic gold and silver nanoparticles on SiO_2 substrate to study light trapping. The BNNPs are used to study bimetallic's effect on the light trapping enhancement as studies show a broader surface plasma spectrum. However, due to the interference effect that might occur in that BNNPs, thus, the deposition thickness, as well as the annealing time, need to be varied to get the optimum condition, such as particles size and interparticle interaction for light trapping. Using the electron beam evaporation technique, we can ensure the nanoparticles' uniformity on the SiO2 substrate. SiO_2 is used in this research due to its semiconductor behavior which is good for photosensor application and can withstand the high annealing temperature of gold and silver NPs (Chen et al., 2016).

Optical characterization was done on the NPs and BNNPs to determine the enhancements in light trapping.

2. Materials and Methods

2.1 Substrates Cleaning

Before any coatings, the glass substrates used (Sail Brand No. 7101 microscope slides) underwent sequential cleaning processes to reduce contamination and remove air particles and dust on the substrates' surface. The substrates were cleaned by sonication using an ultrasonic cleaning machine for 5 min at 25℃with each of the following liquids (1) acetone solution, (2) isopropyl alcohol, and (3) distilled water. Next, the substrates were dried using an air spray gun.

2.2 Fabrication of Au, Ag, and Au-Ag bimetallic NPs

Thin metal films were prepared using the physical vapor deposition method with the aid of an electron beam machine. The manipulating variable in the deposition is the film coating thickness of Au and Ag. The Au and Ag shots act as a target anode and are bombarded with an electron beam given off by a charged tungsten filament under high vacuum conditions to form the samples. The ranges chosen for the Au film are set to be 6nm and 8nm, while the Ag films are set to be 8nm and 10nm. The predefined parameters used to deposit the films are under a pressure of $3\text{x}10^{-6}$ Torr, a deposition rate of 0.3 $\text{Å}/s$, and a deposition voltage of 6.99kV. For each of the depositions, current to the tungsten filament which heats the metal source was slowly tuned to achieve the desired deposition rate. When the deposition rate was stabilized, the main shutter was opened to allow the film coating until the targeted thickness was achieved. The main shutter was closed immediately while the current and voltage were tuned to off subsequently. The samples were taken out from the vacuum chamber after 30 min of cooling to prevent damage to the tungsten filament due to thermal shock. After obtaining the thin films of Au and Ag on the substrates, they were brought to undergo a dewetting process in a furnace with a duration of 1 min under 600℃ and 500℃ respectively to produce the NPs. The Au-Ag bimetallic NPS was produced using the combination steps of producing the Au and Ag NPs. The detailed parameters for the NPS fabrication are shown in Table 1.

2.3 Characterization of Nanoparticles

FEI Quanta 400F scanning electron microscope (FESEM) was used to characterize the Au, Ag, and Au-Ag bimetallic NPs. Surface morphology of the NPs was observed by obtaining high-resolution images down to nanoscale using these instruments. The FESEM images were further processed using ImageJ and Origin to obtain the nanoparticle size distribution. On the other hand, the SPR wavelength and absorption spectra for each of the

NPs were characterized using a Perkin Elmer Lambda 750 UV-Vis Spectrometer.

Table 1: Detail parameters of NPS fabrication.

Samples	Film Coating Thickness (nm)	Deposition rate (A ̊/s)	Dewetting Temperature (°C)	Dewetting Time (min)
Au	6	0.3	600	1
Au	8	0.3	600	1
Ag	8	0.3	500	1
Ag	10	0.3	500	1
Au/Ag	6/8	0.3	600/500	1/1
Au/Ag	8/10	0.3	600/500	1/1

3. Results and Discussion

According to (Basu et al., 2007), the size of Au and Ag nanoparticles affected the surface plasmon resonance of the nanostructure; thus, optical characterization has been done to determine the difference. Different deposition thicknesses will lead to different particle size distribution while the annealing time is kept constant at 1 minute. Therefore, FESEM imaging is first done to see the particle distribution in the nanoparticles. As in Figure 1, the two Au nanoparticles with different deposition thicknesses show not much difference in size. For 6nm deposition, the average nanoparticle size is 32.81319 ± 13.54845 nm while 53.53567 ± 44.00106 nm for 8nm deposition thickness. From this result, the average nanoparticle size for 8nm deposition thickness is bigger than 6nm deposition thickness, but fluctuation is quite high for both nanoparticles, which are 41.29% and 82.19%, respectively. Due to the difference in particle size, a bigger particle size will have a redshift in the UV-Vis absorption spectra (Loewenstein et al., 2008). However, there is no significant redshift shown in the UV-Vis spectra shown in Figure 1. This happens due to the actual size of most particle in 8nm deposition thickness. As we can see in part (d), the histogram shows that most particles in the 8nm deposition thickness nanoparticles have a particle size of approximately ~ 32nm. This explains why the UV-Vis spectra did not give the redshift instead of a very slight blue shift at approximately ~550nm.

As in Figure 2, two silver nanoparticles with different deposition thicknesses of 8nm and 10nm were then characterized. From the result, it can be observed that the average particle size of both silver nanoparticles is quite the same. The 8nm deposition thickness gives 51.23858 ± 18.54225 nm average particle size while 54.25389 ± 22.55314 nm for 10nm

deposition thickness. Besides, the fluctuation for both silver nanoparticles is also quite low, which are 36.19% and 41.57%, respectively. From the histogram also we can find that majority of the particles in both nanoparticles have the size near the average size. There is a slight difference in particle size of both nanoparticles, thus explaining why the UV-Vis spectra have the same absorption peak wavelength. Both nanoparticles seems to have an absorption peak wavelength at approximately ~450nm.

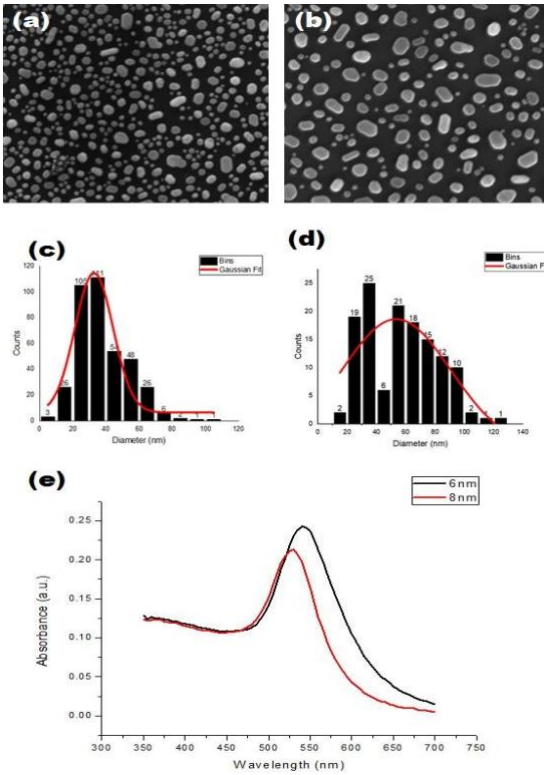

Figure 1: FESEM imaging for Au nanoparticles at (a) 6nm, and (b) 8nm deposition thickness. While the size distribution analysis by histogram for Au nanoparticles at (c) 6nm, and (d) 8nm deposition thickness. Lastly, UV-Vis spectroscopy for Au nanoparticles at 6nm and 8nm.

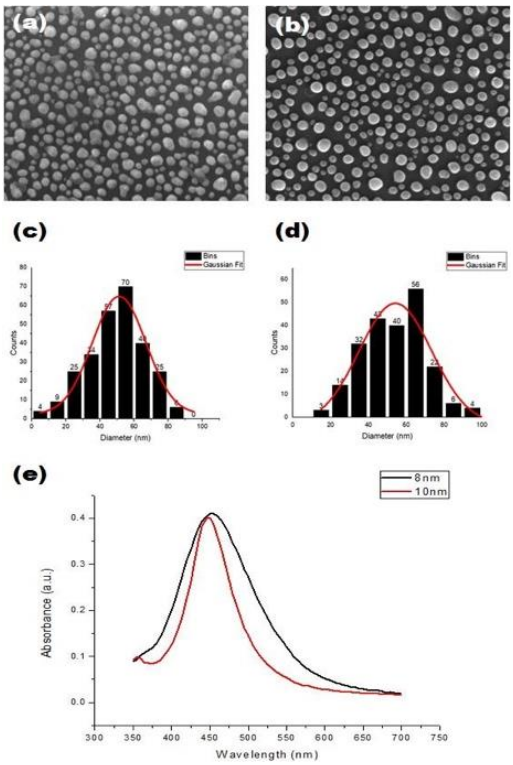

Figure 2: FESEM imaging for Ag nanoparticles at (a) 8nm, and (b) 10nm deposition thickness. While, the size distribution analysis by histogram for Ag nanoparticles at (c) 8nm, and (d) 10nm deposition thickness. Lastly, UV-Vis spectroscopy for Ag nanoparticles at 8nm and 10nm.

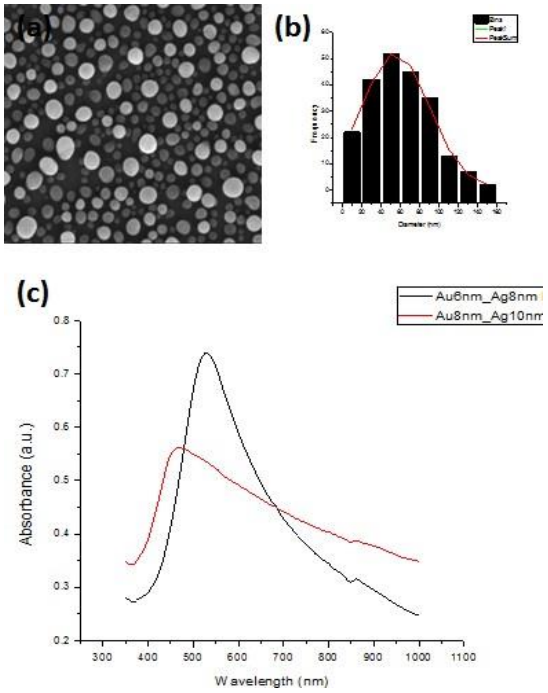

Figure 3: (a) FESEM image for AuAg BNNPs with deposition thickness of 8nm and 10nm, respectively. And (b) particle analysis using ImageJ, (c) UV-Vis spectra for AuAg BNNPs with different deposition thicknesses.

As in Figure 3, the characterization for AuAg BNNPs was obtained. From the imaging result using FESEM, we can differentiate between Au and Ag particles based on their size and contour. By using ImageJ, we identify the mean diameter for this BNNPs at 55nm. However, the particle size distribution is also not very well uniform in this result. But, UV-Vis characterization occurs to have broader spectra than single Au and Ag NPs. This result agrees with the previous study and the need to have a better light trapping ability.

Table 2: Further analysis on the particle distribution

	NPs Diameter Range (Mean) in nm			Distance between NPs (Mean) in nm		
Samples (Deposition Thickness)	**Au NPs**	**Ag NPs**	**Au-Ag BNNPs**	**Au-Au NPs**	**Ag-Ag NPs**	**Au-Ag NPs**
Au NPs (8nm)	14-126 (57.3)			40-252 (102.2)		
Ag NPs (10nm)		4-101 (54.7)			60-180 (107.4)	
AuAg BNNPs (8nm and 10nm)	75-120 (94)	45-90 (58)	45-120 (55)	105-330 (230)	50-105 (72)	65-130 (94)

As tabulated in In table *2*, we manually obtained the mean diameter and distance between particles using ImageJ. We are interested in 8nm deposition thickness of Au and 10nm of Ag. From the table, we can conclude that for all NPS and BNNPs the size distribution is too broad, which means the interaction between particles and the separation is various. These broad results are why the shifting in Figure 1 and Figure 2 do not agree with the previous study.

Conclusion

In conclusion, the UV-Vis absorption spectra show shifting with differences in particle size. However, it is important to have a uniform particle size to observe the shifting effect well. Next, bimetallic nanoparticles also give a broader absorption spectrum compared to a single metallic nanoparticle. This proves that the surface plasmon resonance for Au and Ag does not have much interference for this configuration. Thus, we can conclude that bimetallic nanoparticle is more dependable for selective detection sensor.

Competing interests

The authors declare no conflict of interest

References

[1] R.F. Aroca. Plasmon-enhanced spectroscopy. *Physical Chemistry Chemical Physics*. 2013.

[2] S. Basu, S.K. Ghosh, S. Kundu, S. Panigrahi, S. Praharaj, S. Pande, T. Pal. Biomolecule induced nanoparticle aggregation: Effect of particle size on interparticle coupling. *Journal of Colloid and Interface Science*. 2017: 313;2; 724–734.

[3] F. Canfarotta, M.J. Whitcombe, & S.A. Piletsky. Polymeric nanoparticles for optical sensing. *Biotechnology Advances*. 2013: 31;8; 1585–1599.

[4] J. Chen, W. Tang, B. Tian, B. Liu, X. Zhao, Y. Liu, K.P. Loh. Chemical Vapor Deposition of High-Quality Large-Sized MoS_2Crystals on Silicon Dioxide Substrates. *Advanced Science*. 2016: *3*;8; 1–7.

[5] C. Clavero. Plasmon-induced hot-electron generation at nanoparticle/metal-oxide interfaces for photovoltaic and photocatalytic devices. *Nature Photonics*. 2014: 8;2; 95–103.

[6] S.K. Ghosh & T. Pal. Interparticle coupling effect on the surface plasmon resonance of gold nanoparticles: From theory to applications. *Chemical Reviews*. 2007: 107;11; 4797–4862.

[7] K.S. Lee & M.A. El-Sayed. (2006). Gold and silver nanoparticles in sensing and imaging: Sensitivity of plasmon response to size, shape, and metal composition. *Journal of Physical Chemistry B*. 2006: 110; 39; 19220–19225.

[8] T. Loewenstein, A. Hastall, M. Mingebach, Y. Zimmermann, A. Neudeck, & D. Schlettwein. Textile electrodes as substrates for the electrodeposition of porous ZnO. *Physical Chemistry Chemical Physics*. 2008: 10;14; 1844–1847.

[9] M. Nayeri, M. Moradinasab, & M. Fathipour. The transport and optical sensing properties of MoS2, MoSe2, WS2, and WSe2 semiconducting transition metal dichalcogenides. *Semiconductor Science and Technology*. 2018: 33;2.

[10] A.L. Rogach.Nanocrystalline CdTe and CdTe(S) particles: Wet chemical preparation, size-dependent optical properties, and perspectives of optoelectronic applications. *Materials Science and Engineering B.* 2000: 69; 435–440.

[11] C.L. Tan, S.K Lee, & Y.T. Lee. Bi-SERS sensing and enhancement by Au-Ag bimetallic non- alloyed nanoparticles on an amorphous and crystalline silicon substrate. *Optics Express*. 2015: *23*;5; 6254.

[12] P. Wang, B. Huang, Y. Dai & M.H. Whangbo. (2015). Plasmonic Photocatalysts: Harvesting Visible Light with Noble Metal Nanoparticles. *Physical Chemistry Chemical Physics*. 2015:3:201890; 10715– 10722.

[13] M.D. Ward & A.J. Bard. (1982). Photocurrent enhancement via trapping of photogenerated electrons of TiO2 particles. *Journal of Physical Chemistry*. 1982: 86;18; 3599–3605.

[14] Y. Yang, J. Shi, G. Kawamura & M. Nogami. (2008). Preparation of Au-Ag, Ag-Au core-shell bimetallic nanoparticles for surface-enhanced Raman scattering. *Scripta Materialia*. 2008: 58;10; 862– 865.